

# Nitrogen-rich alkali metal 5,5'-hydrazinebistetrazolate salts: environmentally friendly compounds in pyrotechnic mixtures†

Moritz Ebespächer, Thomas M. Klapötke\* and Carles Miró Sabaté

Received (in Durham, UK) 24th October 2008, Accepted 10th November 2008

First published as an Advance Article on the web 4th December 2008

DOI: 10.1039/b818927g

Straightforward preparations of energetic compounds based on the nitrogen-rich 5,5'-hydrazinebistetrazolate anion ( $[\text{C}_2\text{H}_2\text{N}_{10}]^{2-}$ ) and alkali metals ( $\text{Li}^+$ , **2**,  $\text{Na}^+$ , **3**,  $\text{K}^+$ , **4**,  $\text{Rb}^+$ , **5** and  $\text{Cs}^+$ , **6**) are given by reaction of the free acid 5,5'-hydrazinebistetrazole and a suitable alkali hydroxide or carbonate salts. The new compounds were synthesized in high yields and purities and characterized using analytical (mass spectrometry and elemental analysis) and spectroscopic (IR, Raman and multinuclear NMR) methods. In addition, the solid state structure of the  $[\text{C}_2\text{H}_2\text{N}_{10}]^{2-}$  anion in compounds **2**, **5** and **6** was solved by means of low temperature X-ray crystallography, showing non-coplanar tetrazole rings. Also, the thermal stabilities of the compounds were assessed by differential scanning calorimetry revealing high thermal: stabilities above 215 °C. Initial safety testing gave insight into the low sensitivity of the salts towards impact ( $\geq 30$  J) and friction ( $> 360$  N). Due to the energetic nature of compounds **2–6** the (constant volume) energies of combustion were determined using oxygen bomb calorimetry and were used to calculate the corresponding heats of formation. The response of the compounds in the “flame test” is a burning, deflagration or explosion reaction, depending on the heating mode and the rate of oxidation to the 5,5'-azobistetrazolate ( $[\text{C}_2\text{N}_{10}]^{2-}$ ) derivative. The ready oxidation of the  $[\text{C}_2\text{H}_2\text{N}_{10}]^{2-}$  anion to form the  $[\text{C}_2\text{N}_{10}]^{2-}$  salt provides a safer method for the synthesis of the latter compounds. Lastly, the materials reported here might be of interest as a more environmentally friendly alternative to commonly used compounds in pyrotechnic mixtures.

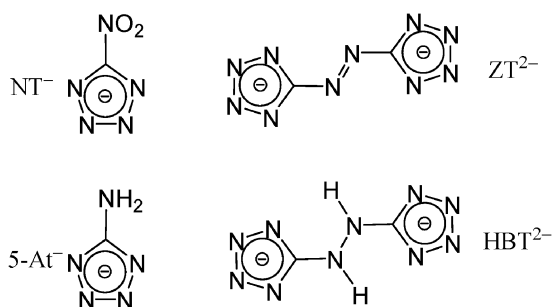
## Introduction

Energetic materials are compounds or mixtures thereof, which are characterized by realizing large amount of hot gaseous products during a short amount of time<sup>1</sup> and have multiple applications familiar to the common public such as their use in fireworks, airbags and fire extinguishers (pyrotechnics),<sup>2,3</sup> rocket or missile fuels (propellants),<sup>4</sup> initiating devices (primary explosives)<sup>5</sup> and rock blasting or building demolition (secondary explosives).<sup>1,6</sup> Polynitrogen chemistry has recently emerged as a milestone in the development of energetic materials.<sup>7–10</sup> Some of the properties of nitrogen-rich compounds, which make them interesting for investigation, are the high average two electron bond energy associated with the nitrogen–nitrogen triple bond, which is a unique feature in the periodic system and makes the compounds energetic. In addition, nitrogen-rich materials will decompose mainly giving off environmentally friendly molecular nitrogen, which is a clear advantage over commonly used energetic compounds (e.g.,  $\text{NH}_4\text{ClO}_4/\text{Al}$ , used as a solid booster in rockets, leads to the

formation of the typical HCl cloud observed during rocket launching).<sup>11</sup> A prominent family of compounds in this regard are azole-based energetic materials.<sup>12–14</sup> When looking at the family of azoles, the nitrogen content and therefore the heat of formation (*i.e.*, the energy content) increases in the direction imidazole ( $\Delta_f H^\circ_{\text{cryst}} = 14.0 \text{ kcal mol}^{-1}$ ),<sup>15</sup> via 1,2,4-triazole ( $\Delta_f H^\circ_{\text{cryst}} = 26.1 \text{ kcal mol}^{-1}$ ) and tetrazole ( $\Delta_f H^\circ_{\text{cryst}} = 56.7 \text{ kcal mol}^{-1}$ ) to pentazole ( $\Delta_f H^\circ_{\text{cryst}} (\text{calc.}) = 110.0 \text{ kcal mol}^{-1}$ );<sup>16</sup> however, the stability of the resulting compounds decreases in the same direction. Triazole- and in particular tetrazole-based materials seem to show the best compromise between high energy content (due to nitrogen catenation) and high thermal and chemical stability (due to aromaticity). In this context, many nitrogen-rich (mainly salt-based) compounds have been synthesized in the last few years, which hold promise for application as propellants or secondary explosives.<sup>17,18</sup> In contrast, metal salts containing a nitrogen-rich cation have been much less widely investigated and also have interesting energetic properties. For example, Hiskey *et al.* studied iron(II) 5-nitrotetrazolate ( $\text{NT}^-$ , Scheme 1) compounds<sup>19</sup> and we synthesized new salts based on the  $\text{NT}^-$  anion and alkali metals,<sup>20</sup> both of which show promise as environmentally friendly primary explosives. Furthermore, metal salts of the 5-aminotetrazolate anion ( $5\text{-AT}^-$ ) burn producing nice flame colours, which suggests their use in fireworks.<sup>21</sup> Metal salts based on the 5,5'-azobistetrazolate anion ( $\text{ZT}^{2-}$ ) generally contain crystal water but when this is removed the compounds

Energetic Materials Research, Department of Chemistry and Biochemistry, University of Munich (LMU), Butenandstr. 5-13, D-81377 Munich, Germany. E-mail: tmk@cup.uni-muenchen.de; Fax: + 49 (0)89 2180 77492

† Electronic supplementary information (ESI) available: X-Ray figures and tables, and pictures of the “flame tests” for compounds **2–6**. CCDC reference numbers 706297–706299. For ESI and crystallographic data in CIF or other electronic format see DOI: 10.1039/b818927g



**Scheme 1** Structural formulas of tetrazolate anions: 5-nitrotetrazolate ( $\text{NT}^-$ ), 5-aminotetrazolate ( $5\text{-AT}^-$ ), 5,5'-azobistetrazolate ( $\text{ZT}^{2-}$ ) and 5,5'-hydrazinebistetrazolate ( $\text{HBT}^{2-}$ ).

become very sensitive and might be used as initiators.<sup>22</sup> In addition, the parent 5,5'-hydrazinebistetrazolate anion ( $\text{HBT}^{2-}$ ) has also been combined with several metals (*e.g.*,  $\text{Hg}^{2+}$ );<sup>23</sup> unfortunately, such compounds generally do not suppose any advantage from the environmental impact point of view in respect of commonly used materials (*e.g.*, lead azide).

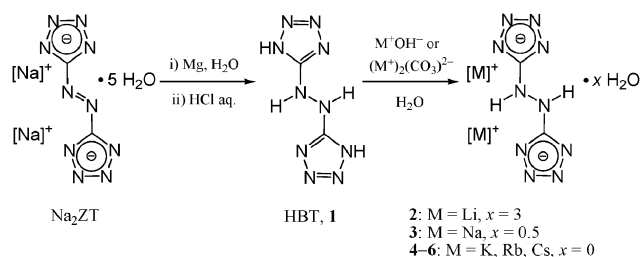
Although neutral 5,5'-azobistetrazole ( $\text{H}_2\text{ZT}$ ) is a very labile compound, which is only stable at temperatures below  $-30\text{ }^\circ\text{C}$ ,<sup>24</sup> the parent 5,5'-hydrazinebistetrazole (HBT) has an unexpectedly great chemical and thermal stability in addition to being a powerful propellant.<sup>9d,25</sup> Therefore, we decided to investigate the energetic properties of salts of HBT with alkaline earth metals,<sup>26</sup> which turned out to have potential for use in pyrotechnics as colour generators. In this second study, we would like to report the synthesis and characterization of salts of HBT with alkali metals and compare their energetic properties with those of alkaline earth metal salts of HBT and with those of alkali metal salts of  $\text{H}_2\text{ZT}$ .

## Results and discussion

### Syntheses

Oxidation of 5-amino-1*H*-tetrazole (5-AT) with potassium permanganate yields sodium 5,5'-azobistetrazolate ( $\text{Na}_2\text{ZT}$ ),<sup>27</sup> which can be isolated as the safe-to-handle pentahydrated species. Reduction of the azo bridge in  $\text{Na}_2\text{ZT}$  with magnesium powder at reflux from water and subsequent acid work-up leads to the formation of HBT (**1**),<sup>9d</sup> which precipitates as a white powder on cooling.

Reaction of **1** with a metal hydroxide or carbonate ( $\text{M}^+\text{OH}^-$ , where  $\text{M}^+ = \text{Li}^+, \text{Na}^+$  and  $\text{K}^+$  or  $(\text{M}^+)_2(\text{CO}_3)^{2-}$ , where  $\text{M}^+ = \text{Rb}^+$  and  $\text{Cs}^+$ ) either in water or in alcoholic solution yielded the corresponding alkali metal salts (**2–6**) according to Scheme 2. The synthesis of compounds **2–6** needs to be carried out under a stream of nitrogen to prevent oxidation of the hydrazine bridge to form the 5,5'-azobistetrazolate salts ( $\text{ZT}^{2-}$ ). However, in the solid state, the stability of the materials towards oxidation is higher (see energetic properties discussion). On the other hand, this offers a new method for the synthesis of  $\text{ZT}^{2-}$  salts, which is safer in comparison to the reported procedure, which makes use of highly sensitive barium 5,5'-azobistetrazolate.<sup>22</sup>



**Scheme 2** Synthesis of alkali metal salts of 5,5'-hydrazinebistetrazole (**2–6**).

### Characterization

Salts **2–6** were characterized by elemental analysis, mass spectrometry and spectroscopic methods (IR, Raman and multinuclear NMR spectroscopy). In some cases, the high nitrogen content of the materials explains the relatively large deviations between calculated and found nitrogen percentages in the elemental analysis of the compounds.

### Spectroscopic discussion

Deprotonation of **1** to form the  $\text{HBT}^{2-}$  anion in compounds **2–6** results in a shift in the resonance of the hydrazine moiety hydrogen atoms to higher field from  $9.62^{25}$  to  $\sim 8.0$  ppm (**2**, **4** and **5**) or  $\sim 7.0$  ppm (**3** and **6**) and the crystal water in the hydrated lithium and sodium salts (**2** and **3**) is observed as a broad resonance at  $\sim 3.8$  ppm. The delocalization of the negative charge in compounds **2–6** produces a deshielding effect on the  $^{13}\text{C}$  NMR resonance of the tetrazolate ring carbon atom, which is observed at low field ( $\sim 168$  ppm) in comparison with the free acid **1** ( $159.6$  ppm).<sup>25</sup> As expected from the quadrupole moment associated with the nucleus, only broad signals were observed in the  $^{14}\text{N}$  NMR of samples of the salts. Also, the low solubility of compounds **2–6** in any solvent tried only allowed to observe the resonance of the hydrazine bridge nitrogen atoms at  $\sim -297$  ppm when recording a  $^{15}\text{N}$  NMR (natural abundance).

As mentioned above, the  $\text{HBT}^{2-}$  anion oxidizes readily to the  $\text{ZT}^{2-}$  anion in solution. Dissolving the pure compounds in  $\text{DMSO}-d_6$  results in a change of colour of the solution from colourless to yellow. The oxidation to the azo compound can be easily monitored by  $^{13}\text{C}$  NMR where the resonance at  $\sim 168$  ppm progressively decreases in intensity over time and instead a new signal at  $\sim 173$  ppm starts to appear. This oxidation is an interesting finding since it influences strongly the energetic properties of the compounds (see energetic properties discussion).

### Vibrational spectroscopy

Vibrational spectroscopy and in particular IR spectroscopy is a powerful tool, not only because it provides qualitative identification of the materials in this work, but also because it gives insight into structural features and hydrogen bonding. On the other hand, vibrational energy calculations provide a good methodology to assign vibrational modes and in particular to identify coupled modes. When the free acid **1** is deprotonated to form compounds **2–6** the changes in the form and shifts of the bands in both the IR and the Raman spectra

are obvious. However, the spectra of the salts **2–6** look very similar among themselves, indicating that the  $\text{HBT}^{2-}$  anion has very similar geometry in all compounds studied, as confirmed by the X-ray crystal structures (see discussion below). Note that the IR and Raman spectra of all five compounds resemble that of the magnesium salt and in both cases the anion has a geometry in which the two tetrazole rings are not coplanar. However, this is in contrast with the rest of the alkaline earth salts (*i.e.*, calcium, strontium and barium), which have clearly different vibrational spectra, and the X-ray structure shows coplanarity between the two tetrazole rings in the anion.<sup>26</sup>

By comparison with the calculated values,<sup>28</sup> the characteristic absorption (IR) and scattering (Raman) bands for the compounds in this study can be easily assigned. In the IR spectra, the X–H region for compounds **2** and **3** is dominated by a broad band corresponding to the O–H stretching of the crystal water and the hydrazine bridge N–H stretches are generally low in intensity with maximum at  $\sim 3200\text{ cm}^{-1}$ . The stretching mode (in-the-plane) between the tetrazole ring carbon atom and the hydrazine bridge nitrogen atom (C1–N5 and C2–N6) is observed as a band of moderate intensity centred at  $\sim 1625\text{ cm}^{-1}$  in the IR spectra and is Raman inactive. The most intense band in the Raman spectra is due to ring stretching modes and is observed at  $\sim 1065\text{ cm}^{-1}$  for the hydrated species (**2** and **3**) and splits into two bands centred at  $\sim 1045$  and  $1085\text{ cm}^{-1}$  for the anhydrous compounds (**4–6**). Note that the band at  $\sim 1045\text{ cm}^{-1}$  and that at  $\sim 1085\text{ cm}^{-1}$  decrease and increase in energy, respectively, in the direction **4**  $\rightarrow$  **6** (**4**,  $1048$  and  $1072\text{ cm}^{-1}$ , **5**,  $1045$  and  $1088\text{ cm}^{-1}$  and **6**,  $1041$  and  $1104\text{ cm}^{-1}$ ). In addition, the in- and out-of-the-plane deformation modes

for the hydrazine bridge nitrogen atoms and the C–N and N–N stretching vibrations are observed in the range  $\sim 1590\text{--}1340\text{ cm}^{-1}$  (IR) and  $\sim 1560\text{--}1370\text{ cm}^{-1}$  (Raman).<sup>29</sup>

Lastly, other signals of lower intensity are present in the vibrational spectra of compounds **2–6**, which can be assigned as follows:  $\sim 1625\text{ cm}^{-1}$  (in-the-plane  $\text{C}_{\text{ring}}\text{--N}_{\text{bridge}}$  stretching),  $\sim 1540\text{--}1510\text{ cm}^{-1}$  (HN–NH deformation and ring C–N stretching),  $\sim 1490\text{--}1440\text{ cm}^{-1}$  (in-the-plane HN–NH deformation and ring N–N stretching),  $\sim 1390\text{--}1360\text{ cm}^{-1}$  (out-of-the-plane HN–NH deformation and ring N–N stretching),  $\sim 1170\text{--}1100\text{ cm}^{-1}$  (ring N–N stretching),  $\sim 1080\text{--}1040\text{ cm}^{-1}$  (ring C–N–N and N–N stretching),  $\sim 1025\text{--}1010\text{ cm}^{-1}$  (ring C–N–N stretching),  $\sim 860\text{--}830\text{ cm}^{-1}$  (in-the-plane HN–NH deformation) and  $\sim 780\text{--}725\text{ cm}^{-1}$  (HN–NH wagging).<sup>9,29</sup>

## Molecular structures

Single crystals of salts **2**, **5** and **6** were obtained as described in the experimental section and the structure of the compounds was determined by X-ray analysis. Data sets were collected on an Oxford Diffraction Xcalibur 3 diffractometer equipped with a CCD detector using the CrysAlis CCD software.<sup>30</sup> The data reduction was performed with the CrysAlis RED software<sup>31</sup> and the structures were solved using the corresponding programs available in the WinGX package<sup>32–35</sup> and finally checked using the program *PLATON*.<sup>36</sup> All non-hydrogen atoms were refined anisotropically, whereas the hydrogen atoms were located from difference Fourier electron density maps and refined isotropically. A *SCALE3 ABSPACK* multi-scan method was used for the absorption correction.<sup>37</sup> Table 1 shows the results of

**Table 1** Crystal structure solution and refinement for salts **2**, **5** and **6**

	<b>2</b>	<b>5</b>	<b>6</b>
Chem. formula	$\text{C}_2\text{H}_8\text{N}_{10}\text{O}_3\text{Li}_2$	$\text{C}_2\text{H}_2\text{N}_{10}\text{Rb}_2$	$\text{C}_2\text{H}_2\text{N}_{10}\text{Cs}_2$
Formula weight/ $\text{g mol}^{-1}$	234.06	337.08	431.96
Crystal size/mm	$0.30 \times 0.20 \times 0.20$	$0.25 \times 0.10 \times 0.05$	$0.35 \times 0.25 \times 0.20$
Crystal system	Triclinic	Monoclinic	Orthorhombic
Space group	$P\bar{1}$	$P2_1/n$	$P2_12_12_1$
$a/\text{\AA}$	6.7522(4)	6.5093(2)	6.0662(1)
$b/\text{\AA}$	7.7880(3)	20.3928(6)	8.5638(2)
$c/\text{\AA}$	10.0091(4)	6.7479(2)	17.8315(4)
$\alpha/^\circ$	83.827(3)	90	90
$\beta/^\circ$	75.925(4)	111.490(4)	90
$\gamma/^\circ$	66.539(4)	90	90
$V/\text{\AA}^3$	468.30(4)	833.46(4)	926.34(3)
$Z$	2	4	4
$\rho_{\text{calc.}}/\text{g cm}^{-3}$	1.660	2.686	3.097
$\mu/\text{mm}^{-1}$	0.139	11.720	7.850
$F(000)$	240	632	776
$\theta$ range/ $^\circ$	4.20–30.11	3.72–25.99	4.06–27.50
$\lambda$ (MoK $\alpha$ )/ $\text{\AA}$	0.71073	0.71073	0.71073
Temp./K	100(2)	100(2)	100(2)
Index range	$-9 \leq h \leq 9$ $-10 \leq k \leq 10$ $-14 \leq l \leq 14$	$-8 \leq h \leq 8$ $-25 \leq k \leq 25$ $-8 \leq l \leq 8$	$-7 \leq h \leq 7$ $-11 \leq k \leq 11$ $-23 \leq l \leq 23$
Refl. collected	13435	8242	10135
Refl. unique	2743	1633	2118
$R$ (int.)	0.0252	0.0251	0.0187
Data/restr./param.	2743/0/186	1633/0/135	2118/0/135
GOOF	1.104	1.026	1.301
$R_1$ , $wR_2$ [ $I > 4\sigma(I)$ ]	0.0316, 0.0898	0.0149, 0.0340	0.0139, 0.0338
$R_1$ , $wR_2$ (all data)	0.0410, 0.0933	0.0209, 0.0363	0.0143, 0.0340
CCDC numbers	706297	706298	706299

**Table 2** Selected bond distances/Å in 5,5'-hydrazinebistetrazole alkali metal salts

Bond	2 (A)	2 (B)	5 (A)	5 (B)	6 (A)	6 (B)
C1–N1	1.342(1)	1.394(1)	1.336(3)	1.400(3)	1.333(4)	1.388(4)
N1–N2	1.359(1)	1.334(1)	1.357(3)	1.335(3)	1.369(4)	1.333(4)
N2–N3	1.303(1)	1.353(1)	1.312(3)	1.361(3)	1.309(4)	1.378(3)
N3–N4	1.358(1)	1.315(1)	1.365(3)	1.320(3)	1.357(4)	1.313(4)
N4–C1	1.337(1)	1.356(1)	1.336(3)	1.355(3)	1.348(3)	1.364(3)
C1–N5	1.375(1)	1.334(1)	1.396(3)	1.335(3)	1.385(4)	1.344(4)
N5–N5 <sup>i</sup>	1.412(1)		1.432(3)		1.416(4)	

**Table 3** Selected bond angles/° in 5,5'-hydrazinebistetrazole alkali metal salts

Angle	2 (A)	2 (B)	5 (A)	5 (B)	6 (A)	6 (B)
N3–N2–N1	109.88(8)	109.65(8)	109.7(2)	109.4(2)	110.4(2)	109.9(2)
N2–N3–N4	109.93(8)	109.62(8)	109.9(2)	109.7(2)	109.4(2)	109.7(2)
N4–C1–N1	112.61(9)	116.04(8)	113.5(2)	113.6(2)	113.1(3)	114.0(2)
N4–C1–N5	125.01(9)	112.94(8)	122.6(2)	115.5(2)	120.1(3)	116.2(3)
N1–C1–N5	122.22(9)	122.66(9)	123.8(2)	123.4(2)	126.8(3)	124.3(3)
C1–N1–N2	103.73(8)	103.91(8)	103.7(2)	103.7(2)	103.2(2)	103.2(2)
C1–N4–N3	103.85(8)	103.77(8)	103.2(2)	103.8(2)	104.0(3)	103.6(2)
C1–N5–N5 <sup>i</sup>	116.04(8)		113.6(2)		114.0(2)	

the crystal structure solution and refinement for compounds **2**, **5** and **6**. A summary of bond distances and angles is found in Table 2 and Table 3, whereas Table 4 presents the hydrogen bonding geometries for all three compounds. Tables S1–S3 from the ESI† contain a tabulated record of the distances for the coordination around the Li<sup>+</sup>, Rb<sup>+</sup> and Cs<sup>+</sup> cations in compounds **2**, **5** and **6**, respectively. CCDC 706297 (**2**), CCDC 706298 (**5**) and CCDC 706299 (**6**).†

The distances and angles for the HBT<sup>2−</sup> anion (Table 2 and Table 3) in compounds **2**, **5** and **6** are, within the limits of the measurement, very similar among the three compounds, which is in agreement with the vibrational spectroscopy results (see discussion above). In general, the C–N and N–N distances for all three salts are longer than those found in neutral **1**.<sup>25</sup>

**Table 4** Hydrogen bonding geometry in 5,5'-hydrazinebistetrazole alkali metal salts

D–H...A	D–H/Å	H...A/Å	D...A/Å	D–H...A/°
<b>2</b>				
N5–H5...N9 <sup>i</sup>	0.87(1)	2.21(1)	2.956(1)	144(1)
N6–H6...N2 <sup>ii</sup>	0.84(1)	2.41(1)	3.142(1)	145(1)
O3–H3B...N9 <sup>iii</sup>	0.87(2)	2.06(2)	2.845(1)	149(2)
O3–H3B...N10 <sup>iii</sup>	0.87(2)	2.67(2)	3.233(1)	123(1)
O2–H2B...N10 <sup>i</sup>	0.84(2)	2.02(2)	2.838(1)	166(2)
O1–H1A...N1 <sup>ii</sup>	0.83(2)	2.14(2)	2.963(1)	177(2)
O3–H3A...N2 <sup>iv</sup>	0.88(2)	1.92(2)	2.794(1)	173(2)
O1–H1B...N1 <sup>v</sup>	0.87(2)	2.07(2)	2.933(1)	169(2)
O2–H2A...O1 <sup>vi</sup>	0.85(2)	2.04(2)	2.859(1)	163(2)
<b>5</b>				
N5–H5...N8 <sup>i</sup>	0.75(2)	2.51(2)	3.246(3)	167(2)
N5–H5...N7 <sup>i</sup>	0.75(2)	2.51(2)	3.179(3)	149(2)
N6–H6...N9 <sup>ii</sup>	0.84(3)	2.58(3)	3.104(3)	122(2)
<b>6</b>				
N5–H5...N2	0.83(4)	2.27(4)	3.024(3)	153(3)
N6–H6...N4 <sup>i</sup>	0.82(4)	2.24(4)	3.060(4)	172(4)

Symmetry codes for **2**: (i)  $-x, 1-y, 1-z$ ; (ii)  $-x, 1-y, 2-z$ ; (iii)  $1-x, 1-y, 1-z$ ; (iv)  $1-x, -y, 2-z$ ; (v)  $x, 1+y, z$ ; (vi)  $x, -1+y, z$ . **5**: (i)  $0.5+x, 0.5-y, 0.5+z$ ; (ii)  $0.5+x, 0.5-y, -0.5+z$ . **6**: (i)  $2-x, 0.5+y, 1.5-z$ .

Both C–N and N–N distances have values that are between those of classical single bonds and those of classical double bonds<sup>38</sup> indicating that the negative charge is extensively delocalized around the tetrazole rings.

The lithium salt (**2**) crystallizes with three molecules of crystal water by analogy with lithium 5-nitrotetrazolate.<sup>20</sup> Both crystallographically independent lithium atoms (Li1 and Li2) in the asymmetric unit have a coordination number of four (Fig. 1), in keeping with other lithium salts.<sup>39</sup> Li1 has three contacts to nitrogen atoms and one to an oxygen atom of a water molecule, whereas Li2 is coordinated by three water molecules and has one contact to a nitrogen atom of an HBT<sup>2−</sup> anion and both Li<sup>+</sup> cations show distorted tetrahedral geometries. Table S1 (ESI†) summarized the distances and angles for the coordination around the two metal centres. The Li–N and Li–O distances are in the range of 1.9–2.1 Å, as expected, although there exists a longer contact to a nitrogen atom (Li1–N9<sup>ii</sup> and Li2–N5 ~2.8 Å; symmetry code: (ii)  $1-x, 1-y, 1-z$ ). Fig. S1 from the ESI† shows a view of the packing in the unit cell of the compound. In contrast to the 5,5'-azobistetrazolate analogue, where the anion is planar and the compound crystallizes forming layers, the two

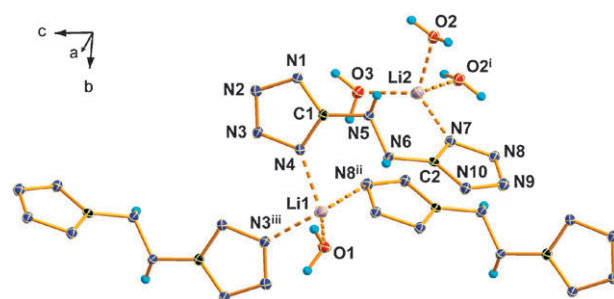


**Fig. 1** Coordination around the Li<sup>+</sup> cations in the crystal structure of **2** and labelling scheme. The long Li–N contacts (~2.8 Å) have been omitted for the sake of simplicity. Symmetry codes: (i)  $1-x, -y, 1-z$ ; (ii)  $1-x, 1-y, 1-z$ ; (iii)  $1-x, 1-y, 2-z$ .



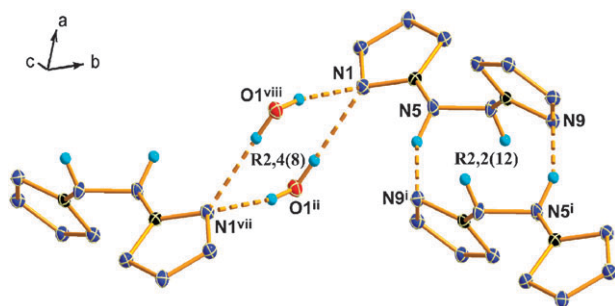


**Fig. 2** Characteristic hydrogen bonding ring graph-sets in the crystal structure of **2**. Symmetry codes: (i)  $-x, 1-y, 1-z$ ; (ii)  $-x, 1-y, 2-z$ ; (vii)  $-x, -y, 2-z$ ; (viii)  $x, -1+y, z$ .

tetrazole rings in **2** are bent in respect to each other ( $C1-N5-N6-C2 = -140.1(1)^\circ$ ).

In addition to contacts to the  $Li^+$  cations, there exist many hydrogen bonds in the structure of **2** (Table 4). These can be best described using the graph-set formalism from Bernstein *et al.*<sup>40</sup> in combination with the *RPLUTO* software.<sup>41</sup> At the primary level there exist seven dimeric **D1,1(2)** and two ring **R2,2(12)** graph-sets, which combine at the secondary level to form many **D1,2(3)**, **D2,2(X)** ( $X = 4, 5, 8, 9$ ), **D2,3(9)** and **D3,3(X)** ( $X = 9, 13, 15$ ) finite patterns, chain **C2,2(X)** ( $X = 10-12$ ) graph-sets and, more interestingly, ring **R2,1(3)** and **R2,4(8)** hydrogen-bonded networks. Fig. 2 shows a **R2,4(8)** and a **R2,2(12)** ring graph-set formed by two HBT<sup>2-</sup> anions and bridging water molecules ( $O1 \cdots N1^{ii} = 2.963(1) \text{ \AA}$ ,  $O1 \cdots N1^v = 2.933(1) \text{ \AA}$ ; symmetry codes: (ii)  $-x, 1-y, 2-z$ ; (v)  $x, 1+y, z$ ) and by two HBT<sup>2-</sup> anions ( $N5 \cdots N9^i = 2.956(1) \text{ \AA}$ ; symmetry code: (i)  $-x, 1-y, 1-z$ ), respectively.

In contrast to the lithium salt, the rubidium derivative (**5**) does not contain crystal water in the structure. This and the larger size of the cation are reflected in the differences in the packing and the larger cell of the rubidium salt ( $833(1) \text{ \AA}^3$  vs.  $468(1) \text{ \AA}^3$ ), respectively. Every single ring nitrogen atom in the HBT<sup>2-</sup> anion of **5** is involved in coordination to  $Rb^+$  cations. Fig. 3 shows a view of the coordination around one of the two crystallographically independent cations ( $Rb1$ ).  $Rb1$  has a coordination number of nine with distances to the metal centre in the range  $Rb1-N \sim 3.00-3.22 \text{ \AA}$  with the next nitrogen atom ( $N9$ ) placed at  $3.465(2) \text{ \AA}$ , whereas  $Rb2$  shows nine contacts with distances in the range  $Rb2-N \sim 2.95-3.26 \text{ \AA}$  and two not significantly longer interactions to  $N1$  and  $N3$  at  $3.360(2)$  and  $3.324(2) \text{ \AA}$ , respectively (Table S2, ESI†).

The dihedral angle  $C1-N5-N6-C2$  with a value of  $83.8(3)^\circ$  indicates non-coplanarity between the two tetrazole rings as also observed for compounds **2** and **6**. The torsion of the two tetrazolate rings is also decisive in conditioning the packing (Fig. 4). The tetrazolate rings with the labels  $C2$  to  $N10$  form layers along a direction that cuts the  $a$ -axis at an angle of  $\sim 20^\circ$  and are connected among them by hydrogen bonds *via* one of the hydrazine bridge nitrogen atoms with  $N6 \cdots N9^{ii} = 3.104(3) \text{ \AA}$  (symmetry code: (ii)  $0.5+x, 0.5-y, -0.5+z$ ) describing **C1,1(6)** chain graph-sets. Three weak ( $3.10-3.25 \text{ \AA}$ ) hydrogen bonds are formed in total. In addition to the aforementioned hydrogen bond, the other hydrazine

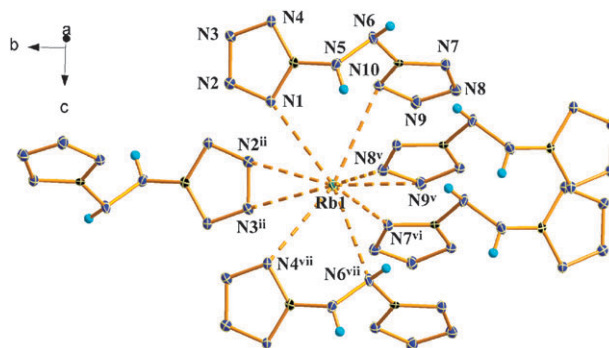


**Fig. 3** Coordination around the  $Rb^+$  cations ( $Rb1$ ) in the crystal structure of **5** and labelling scheme. Symmetry codes: (ii)  $-x, 1-y, 2-z$ ; (v)  $0.5+x, 0.5-y, 0.5+z$ ; (vi)  $-0.5+x, 0.5-y, 0.5+z$ ; (vii)  $x, y, 1+z$ .

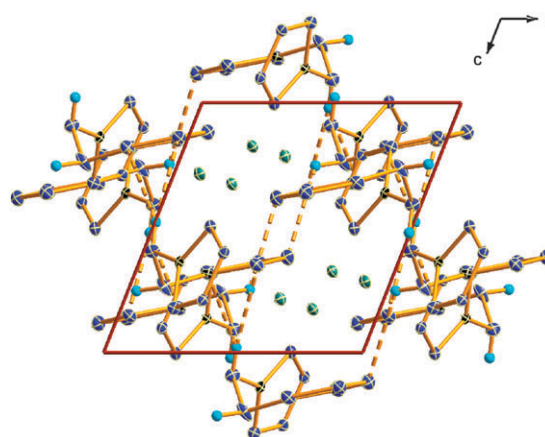


**Fig. 4** Layers formed by the tetrazolate rings and hydrogen bonding (dotted lines) in the unit cell of **5** (view along the  $b$ -axis).

bridge nitrogen atom ( $N5$ ) forms two other hydrogen bonds, which describe **C1,1(5)** chain graph-sets, at the primary level. At the secondary level, **C2,2(X)** ( $X = 6, 7, 10, 11$ ) motifs and one **R2,1(3)** ring network are being formed. For example, the latter is described by the hydrogen bridges formed by  $N5$  and two (almost equidistant) nitrogen atoms belonging to the same tetrazolate ring ( $N5 \cdots N8^i = 3.246(3)$  and  $N5 \cdots N7^i = 3.179(3) \text{ \AA}$ ; symmetry code: (i)  $0.5+x, 0.5-y, 0.5+z$ ).

Caesium 5,5'-hydrazinebistetrazolate (**6**) is one of the few examples of a caesium salt with an azolate anion known in the literature, which has been structurally characterized.<sup>21,42</sup> The two halves of the anion and the two  $Cs^+$  cations are crystallographically independent and are linked to each other by coordination. As represented in Fig. 5 both of the two caesium atoms are surrounded by five anions.  $Cs1$  has a coordination number (CN) of  $10+2$  with ten distances to the nitrogen atoms in the range of  $3.2-3.4 \text{ \AA}$  and two longer contacts at  $\sim 3.7 \text{ \AA}$  (not represented in Fig. 5 for simplicity purposes), whereas  $Cs2$  interacts with the anions at distances of  $3.1-3.5 \text{ \AA}$  with a CN of 11 (Table S3, ESI†). Fig. 6a shows a view of the unit cell of the compound along the  $b$ -axis where there is no evidence of aromatic  $\pi-\pi$  stacking between tetrazole rings. The tetrazole rings belonging to one anion, with torsion angles  $C1-N5-N6-C2 = 83.4(3)^\circ$ , are almost

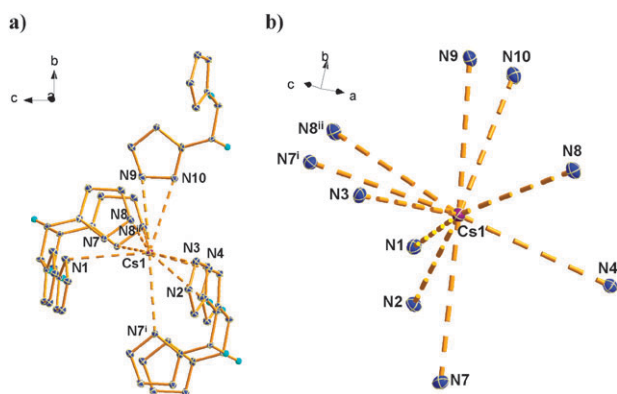


**Fig. 5** (a) Full and (b) simplified coordination around one of the  $\text{Cs}^+$  cations ( $\text{Cs1}$ ) in the crystal structure of **6**. Symmetry codes: (i)  $-0.5 + x, 0.5 - y, 2 - z$ ; (ii)  $-1 + x, y, z$ .

perpendicular, similar to the rubidium salt (**5**) and contrary to the (trihydrated) lithium compound (**2**) and polyhydrated metal salts of the  $\text{HBT}^{2-}$  anion.<sup>26</sup>

In addition to the contacts to the metal, there exist two hydrogen bonds ( $\text{N5} \cdots \text{N2} = 3.024(3)$ ,  $\text{N6} \cdots \text{N4}^i = 3.060(4)$  Å; symmetry code: (i)  $2 - x, 0.5 + y, 1.5 - z$ ) by using the hydrazine bridge hydrogen atoms of one anion well within the sum of the van der Waals radii ( $r_{\text{N}} + r_{\text{N}} = 3.10$  Å),<sup>43</sup> which describe two **C1,1(5)** chain motifs at the primary level and **C2,2(X)** ( $X = 7, 10$ ) graph-sets at the secondary. Also identified by the program *RPLUTO*, four anions combine through hydrogen bonding to form a ring graph-set with the label **R4,4(17)**, again at the secondary level (Fig. 6b). Lastly, the distances and coordination numbers around the metal

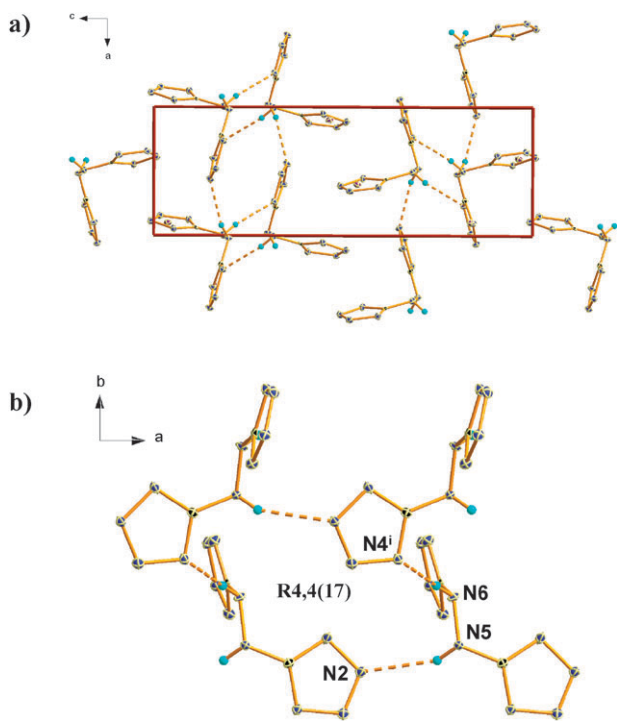


**Fig. 6** (a) Hydrogen bonding in the unit cell (view along the  $b$ -axis) and (b) **R4,4(17)** hydrogen bonding network in the crystal structure of **6**. Symmetry code: (i)  $2 - x, 0.5 + y, 1.5 - z$ .

centres in compounds **2**, **4** and **6** are in agreement with previously reported metal salts with azole-based anions.<sup>20,21,42</sup>

### Energetic properties of metal salts of **1**

Due to the high nitrogen content and highly endothermic character of the  $\text{HBT}^{2-}$  anion, metal salts of **HBT (1)** are potentially energetic compounds. Therefore, it is useful to assess the energetic properties of compounds **2–6** and compare them with those of commonly used compounds or those of other new energetic materials.

In order to assess the hazards involved in the manipulation of the compounds in this study, so-called standard BAM tests<sup>44–49</sup> were used to determine the sensitivity of the salts towards impact and friction using a drop-hammer and a friction tester, respectively. The results of these experiments are tabulated in Table 5 together with other physico-chemical properties of interest. According to our tests, none of the compounds turned out to be sensitive either to impact ( $\geq 30$  J) or to friction ( $> 360$  N) and are thus safe for transport under the UN Recommendations on the Transport of Dangerous Goods, as indicated in ref. 49 (salts **3–6** only showed non-explosive decomposition at 30 J). Also, no explosion was observed when submitting the compounds to the electrostatic discharge of a Tesla coil (ESD testing) nor when grinding them in a mortar. These results are in contrast with those observed for metal salts of the 5,5'-azobistetrazolate anion ( $\text{ZT}^{2-}$ ).<sup>22</sup> Whereas compounds containing the  $\text{ZT}^{2-}$  anion are more prone to contain crystal water, which makes them insensitive towards the above-mentioned stimuli but expected to have sensitivity values comparable to primary explosives as the anhydrous materials (e.g., barium 5,5'-azobistetrazolate), the heavier alkali metal salts containing the  $\text{HBT}^{2-}$  anion (**4–6**) do not incorporate crystal water and are regarded as insensitive or less sensitive compounds. In comparison with commonly used energetic compounds such as TNT or metal-based materials such as lead azide, the compounds described here are less sensitive to both impact and friction.<sup>3</sup>

Differential scanning calorimetry (DSC) was used to assess the thermal stability of the salts **2–6**. The crystal water in the hydrated compounds **2** and **3** is less tightly coordinated to the metal than in alkaline earth metal salts of **1**<sup>26</sup> and is already lost at temperatures of  $\sim 120$  °C (DSC onset). The lithium salt (**2**) is the only material which melts ( $\text{mp} = 191$  °C) with almost concomitant decomposition at  $\sim 216$  °C, whereas the rest of the compounds decompose without melting at or above 230 °C. These decomposition temperatures are generally higher than those measured for analogous salts based on the 5-amino-1*H*-tetrazolate<sup>21</sup> and 5,5'-azobistetrazolate<sup>22</sup> anions. The thermo-gravimetric analysis (TG) for compound **2** agrees well with the DSC results (Fig. 7). The loss of the three molecules of crystal water amounts to 22.85% (2.331 mg) of the original sample (calculated: 23.07%). The decomposition at  $\sim 216$  °C results in a second loss of weight of 59.37% (6.057 mg) so that the residue left (1.814 mg) adds to 17.78% of the original sample. The weight of the residue after the first decomposition step is still larger than what would be expected for the formation of  $\text{Li}_2\text{O}$  (1.302 mg, 12.76%) and a second

**Table 5** Physico-chemical properties of alkali metal salts of **1** (the explosive properties of the anhydrous forms of **2** and **3** were not tested)

	<b>2</b>	<b>3</b>	<b>4</b>	<b>5</b>	<b>6</b>
Formula	C <sub>2</sub> H <sub>8</sub> N <sub>10</sub> Li <sub>2</sub> O <sub>3</sub>	C <sub>2</sub> H <sub>3</sub> N <sub>10</sub> Na <sub>2</sub> O <sub>0.5</sub>	C <sub>2</sub> H <sub>2</sub> N <sub>10</sub> K <sub>2</sub>	C <sub>2</sub> H <sub>2</sub> N <sub>10</sub> Rb <sub>2</sub>	C <sub>2</sub> H <sub>2</sub> N <sub>10</sub> Cs <sub>2</sub>
MW (g mol <sup>-1</sup> )	234.11	221.03	243.97	335.87	431.86
Impact (J) <sup>a</sup>	> 30	~ 30	~ 30	~ 30	~ 30
Friction (N) <sup>a</sup>	> 360	> 360	> 360	> 360	> 360
Electrostatics <sup>b</sup>	—	—	—	—	—
Flame slow heat. <sup>c</sup>	Defl.	Defl.	Exp.	Exp.	Exp.
Flame fast heat. <sup>c</sup>	Burn.	Burn.	Defl.	Defl.	Defl.
Flame colour	Red	Orange	Purple	Lilac	Pink
N (%) <sup>d</sup>	59.9	63.4	57.3	41.6	32.4
Ω (%) <sup>e</sup>	−47.8	−50.7	−45.9	−33.3	−25.9
Endo. (°C) <sup>f</sup>	124 (−H <sub>2</sub> O), 191 (mp)	~ 110 (−H <sub>2</sub> O)–	—	—	—
Dec. (°C) <sup>g</sup>	216, 324	262, 300	236	230	240
−Δ <sub>c</sub> U (cal g <sup>-1</sup> ) <sup>h</sup>	2460(20)	1960(20)	1970(40)	1210(30)	1060(20)
−Δ <sub>c</sub> H° (kJ mol <sup>-1</sup> ) <sup>i</sup>	2400(20)	1800(20)	2010(40)	1690(30)	1910(20)
Δ <sub>f</sub> H° (kJ mol <sup>-1</sup> ) <sup>j</sup>	−120(100)	80(90)	−370(160)	345(110)	280(80)

<sup>a</sup> Impact and friction sensitivities determined by standard BAM methods (see ref. 44–49). <sup>b</sup> Rough sensitivity to 20 kV electrostatic discharge (ESD testing): + sensitive, – insensitive from an HF-Vacuum-Tester type VP 24. <sup>c</sup> Response to fast heating in the “flame test” (“slow and fast heating”): burn. (burning), defl. (deflagration) or expl. (explosion). <sup>d</sup> Nitrogen content. <sup>e</sup> Oxygen balance, calculated according to ref. 50. <sup>f</sup> Endothermic peaks (*i.e.*, melting or water loss) and decomposition point (DSC onset) from measurement with  $\beta = 5^\circ\text{C min}^{-1}$ . <sup>g</sup> Endothermic peaks (*i.e.*, melting or water loss) and decomposition point (DSC onset) from measurement with  $\beta = 5^\circ\text{C min}^{-1}$ . <sup>h</sup> Experimental (constant volume) energy of combustion. <sup>i</sup> Experimental molar enthalpy of combustion. <sup>j</sup> Molar enthalpy of formation.

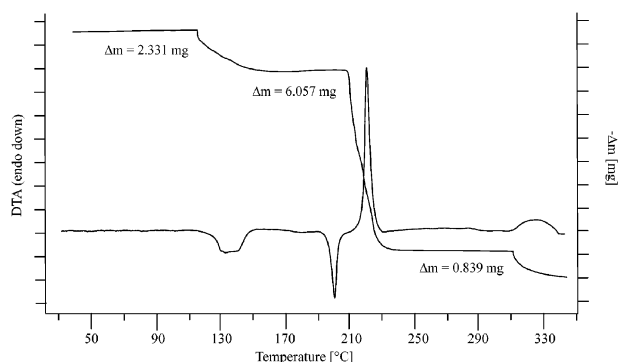


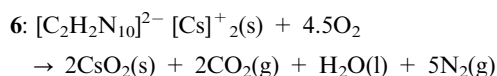
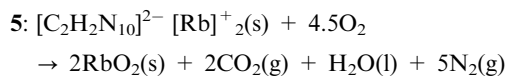
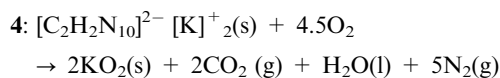
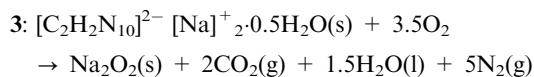
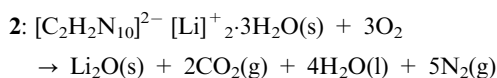
**Fig. 7** TG curve of compound **2** with the DTA curve (left axis) and the loss of mass (right axis). Measurement at  $\beta = 5^\circ\text{C min}^{-1}$  (initial sample weight = 10.202 mg).

decomposition step at  $\sim 321^\circ\text{C}$  results in the loss of further 8.22% weight (0.839 mg).

In addition to DSC and TG analysis, all alkali metal salts were tested in the “flame test” using two heating modes. In the “slow heating” mode, a few milligrams of the compound to be tested were placed on a thick metal spatula  $\sim 5$  cm above the flame of a Bunsen burner, whereas in the “fast heating flame test” the compound was loaded on a thin spatula, which was put into direct contact with a flame. Pictures of these two tests can be found in the supporting information (Fig. S2, ESI†). “Slow heating” of alkali metal salts **2–6** resulted in deflagration with little smoke (**2**, accompanied by red colour) and low (**3** and **4**) or loud (**5** and **6**) explosions. On the other hand, “fast heating” resulted in a less violent reaction, which is exactly the opposite behaviour to that exhibited by alkaline earth salts of **1**.<sup>26</sup> **2** and **3** burned nicely with almost no smoke producing a red and an orange flame, respectively, whereas the heavier alkali metal salts (**4–6**) showed a more violent response deflagrating giving the typical colour for the metal cation, namely purple, lilac and pink. This is an interesting finding

since these results are in agreement with the higher sensitivity towards oxidation of the heavier alkali metal salts (**4–6**). Whereas powders of the hydrated salts **2** and **3** are stable in air for several weeks without appreciable oxidation, compounds **4–6** oxidize readily to the yellow 5,5'-azobistetrazolate salts after a few hours of contact with air. Thus, we assume that heating in the flame accelerates the process of oxidation to the azo derivatives, for which the expected response in the “flame test” is an explosion.<sup>22</sup> An explanation for this observation can be that the crystal water stabilizes the materials and prevents oxidation, which fits in with the low susceptibility of alkaline earth salts of **1** towards oxidation (all contain  $\geq 5$  molecules of crystal water and are stable, at least, for several months).<sup>26</sup>

In addition to safety aspects, thermodynamic parameters are also of interest to assess the energetic properties of the compounds in this work. Due to the energetic nature of the HBT<sup>2-</sup> anion, the constant volume energies of combustion ( $\Delta_c U$ ) of the alkali metal salts **2–6** were measured using oxygen bomb calorimetry. The equation  $\Delta_c H^\circ = \Delta_c U + \Delta n RT$  (where  $\Delta n$  is the difference between the number of moles of gases in the products and the reactants) was used to calculate the standard molar enthalpies of combustion ( $\Delta_c H^\circ$ ). The standard energies of formation of salts **2–6** ( $\Delta_f H^\circ$ ) were back-calculated from the energy of combustion on the basis of the combustion equations shown below, Hess’s law and the known standard heats of formation for Li<sub>2</sub>O, Na<sub>2</sub>O<sub>2</sub>, MO<sub>2</sub> (M = K, Rb, Cs), water and carbon dioxide.<sup>51</sup> The energies of combustion, obtained as averaged values from sets of four measurements (Table 5), are generally more negative than those of alkali metal salts of 5-amino-1H-tetrazole<sup>21</sup> and the standard heats of formation are accordingly more positive (less negative) in keeping with the less negative oxygen balance of the compounds reported here. The oxides chosen in the following equations were based on the atmospheric combustion chemistry of the alkali metals and have not been identified analytically.



## Experimental section

**Caution!** Although we have experienced no difficulties in handling the compounds described in this work, tetrazoles and their derivatives are energetic materials and tend to explode under certain conditions. Although the explosive properties of salts **2–6** have been assessed herein, they have not been fully established yet. We therefore recommend that the synthesis is carried out only by expert personnel, wearing protective gear (*i.e.*, Kevlar gloves, wrist protectors, leather jacket, helmet, ear plugs, ...) and using conductive equipment, specially when working on a larger scale.

### General

All chemical reagents and solvents were obtained from Sigma-Aldrich Inc. or Acros Organics (analytical grade) and were used as supplied. Sodium 5,5'-azobistetrazolate pentahydrate was prepared according to a literature known procedure<sup>27</sup> and used to prepare HBT (**1**). Melting points were determined by DSC (Linseis DSC PT-10 instrument<sup>52</sup> calibrated with standard pure indium and zinc). Measurements were performed in closed aluminium sample pans with a 1  $\mu\text{m}$  hole in the top for gas release under a nitrogen flow of 20  $\text{mL min}^{-1}$  with an empty identical aluminium sample pan as a reference. Infrared (IR) spectra were recorded on a Perkin-Elmer Spectrum One FT-IR instrument as KBr pellets at 20  $^\circ\text{C}$ .<sup>53</sup> Transmittance values are qualitatively described as “very strong” (vs), “strong” (s), “medium” (m) and “weak” (w). Raman spectra were recorded on a Perkin-Elmer Spectrum 2000R NIR FT-Raman instrument equipped with a Nd : YAG laser (1064 nm). The intensities are reported as percentages of the most intense peak and are given in parentheses.  $^1\text{H}$  and  $^{13}\text{C}$  NMR spectra were recorded on a JEOL Eclipse 400 instrument in  $\text{DMSO}-d_6$  at or near 25  $^\circ\text{C}$ . The chemical shifts are given relative to tetramethylsilane as

external standard. Lastly, elemental analyses were performed with a Netsch Simultaneous Thermal Analyzer STA 429.

### Bomb calorimetry

For the calorimetric measurements of the metal salts **2–6** a Parr 1356 bomb calorimeter (static jacket) equipped with a Parr 207A oxygen bomb for the combustion of highly energetic materials was used.<sup>54</sup> A Parr 1755 printer, furnished with the Parr 1356 calorimeter, was used to produce a permanent record of all activities within the calorimeter. The samples ( $\sim 200$  mg each) were carefully mixed with  $\sim 800$  mg analytical grade benzoic acid and carefully pressed into pellets, which were subsequently burned in a 3.05 MPa atmosphere of pure oxygen. The experimentally determined constant volume energies of combustion ( $\Delta_c U(\text{exp})$ ) were obtained as the averages of four single measurements with standard deviations calculated as a measure of experimental uncertainty. The calorimeter was calibrated by the combustion of certified benzoic acid in an oxygen atmosphere at a pressure of 3.05 MPa.

### Synthesis of HBT (**1**)

**1** was synthesized according to a recently reported procedure in our group<sup>9d</sup> in a 97% yield. DSC (5  $^\circ\text{C min}^{-1}$ ,  $^\circ\text{C}$ ): 207 (dec.);  $\text{C}_2\text{H}_4\text{N}_{10}$  (168.12  $\text{g mol}^{-1}$ ) calc.: C 14.29, H 2.40, N 83.31%; found: C 14.18, H 2.31, N 82.73%.

### Synthesis of lithium 5,5'-hydrazinebistetrazolate trihydrate (**2**)

Lithium hydroxide (0.096 g, 4.0 mmol) was dissolved in 10 mL of oxygen-free water, degassed by bubbling nitrogen gas through it over  $\sim 15$  min. Neat **1** (0.336 g, 2.0 mmol) was added portion-wise under a stream of nitrogen. After 15 min reaction time all the insoluble material had dissolved yielding a clear colourless solution. This was heated briefly to reflux and the solvent was removed under high vacuum and at 50  $^\circ\text{C}$  yielding the lithium salt as a white powder in nearly quantitative yield (0.457 g). Single crystals of the product suitable for X-ray analysis were obtained by slow evaporation of a water solution of the compound under a nitrogen flow. DSC (5  $^\circ\text{C min}^{-1}$ ,  $^\circ\text{C}$ ):  $\sim 124$  ( $-\text{H}_2\text{O}$ ),  $\sim 191$  (mp), 216, 324 (dec.); IR (KBr,  $\text{cm}^{-1}$ )  $\tilde{\nu} = 3498(\text{m})$ , 3292(w), 3251(w), 3200(vw), 2993(w), 2888(vw), 1641(m), 1625(m), 1573(s), 1527(m), 1489(w), 1409(vw), 1366(vs), 1273(w), 1248(w), 1217(w), 1154(w), 1135(w), 1128(w), 1109(vw), 1071(w), 1061(vw), 1019(w), 999(w), 850(vw), 758(vw), 733(m), 683(w), 650(vw), 628(vw), 609(w); Raman (400 mW, 25  $^\circ\text{C}$ ,  $\text{cm}^{-1}$ )  $\tilde{\nu} = 3294(22)$ , 3252(20), 1638(14), 1609(23), 1583(14), 1537(73), 1487(24), 1409(11), 1367(28), 1287(13), 1274(18), 1249(52), 1219(32), 1177(12), 1137(41), 1085(35), 1072(100), 1049(46), 1023(22), 857(28), 762(15), 675(8), 572(9), 392(26), 374(19), 348(18), 236(24), 171(54);  $^1\text{H}$  NMR ( $\text{DMSO}-d_6$ , 25  $^\circ\text{C}$ , ppm)  $\delta$  8.00 (s, 2H, NH–NH), 3.83 (s,  $\sim 6\text{H}$ ,  $\text{H}_2\text{O}$ );  $^{13}\text{C}$  NMR ( $\text{DMSO}-d_6$ , 25  $^\circ\text{C}$ , ppm)  $\delta$  167.8 (2C,  $\text{C}_{\text{ring}}$ );  $m/z$  (FAB<sup>–</sup>, xenon, 6 keV, glycerine matrix): 84.0 (4,  $[\text{CH}_2\text{N}_5]^-$ ), 118.1 (3,  $\text{HCN-gly}$ ), 124.1 (3,  $[\text{C}_2\text{H}_2\text{N}_7]^-$ ), 166.0 (5,  $[\text{C}_2\text{H}_2\text{N}_{10}]^{2-}$ ), 167.0 (29,  $[\text{C}_2\text{H}_3\text{N}_{10}]^-$ ), 173.0 (12,  $[\text{C}_2\text{H}_2\text{N}_{10}\text{Li}]^-$ ), 189.1 (9,  $[\text{C}_2\text{H}_2\text{N}_{10}\text{LiO}]^{3-}$ ), 259.1 (7,  $\text{C}_2\text{H}_4\text{N}_{10}\text{-gly}$ ), 265.0 (6,  $\text{C}_2\text{H}_3\text{N}_{10}\text{Li-gly}$ ), 271.1 (3,  $\text{C}_2\text{H}_2\text{N}_{10}\text{Li}_2\text{-gly}$ );  $\text{C}_2\text{H}_8\text{N}_{10}\text{O}_3\text{Li}_2$



(234.11 g mol<sup>-1</sup>) calc.: C 10.25, H 3.44, N 59.81%; found: C 10.96, H 3.58, N 63.19%.

### Synthesis of sodium 5,5'-hydrazinebistetrazolate hemihydrate (3)

**1** (0.336 g, 2.0 mmol) was suspended in 10 mL degassed water (see synthesis of compound **2**) and reacted with neat sodium hydroxide (0.160 g, 4.0 mmol) under a flow of nitrogen. After ~20 min reaction time a light clear yellow solution formed and the solvent was removed under high vacuum leaving behind a light yellow powder of the compound, which could be recrystallized from dry ethanol–water (0.416 g, 80%). DSC (5 °C min<sup>-1</sup>, °C): ~110 (–H<sub>2</sub>O), 262, 300 (dec.); IR (KBr, cm<sup>-1</sup>)  $\tilde{\nu}$  = 3457(m), 3228(m), 1632(vw), 1549(s), 1474(vs), 1360(s), 1218(w), 1118(s), 1062(w), 1010(m), 833(w), 762(w); Raman (400 mW, 25 °C, cm<sup>-1</sup>)  $\tilde{\nu}$  = 3428(2), 3198(14), 1566(27), 1511(16), 1390(18), 1245(45), 1231(12), 1144(8), 1120(22), 1060(100), 1008(6), 939(9), 780(10), 705(10), 543(4), 400(13), 371(11), 222(19); <sup>1</sup>H NMR (DMSO-*d*<sub>6</sub>, 25 °C, ppm)  $\delta$  6.91 (s, 2H, NH–NH), 3.92 (s, ~1H, H<sub>2</sub>O); <sup>13</sup>C NMR (DMSO-*d*<sub>6</sub>, 25 °C, ppm)  $\delta$  167.6 (2C, C<sub>ring</sub>); *m/z* (FAB<sup>–</sup>, xenon, 6 keV, glycerine matrix): 84.0 (6, [CH<sub>2</sub>N<sub>5</sub>]<sup>–</sup>), 118.1 (3, HCN-gly), 124.1 (2, [C<sub>2</sub>H<sub>2</sub>N<sub>7</sub>]<sup>–</sup>), 166.0 (8, [C<sub>2</sub>H<sub>2</sub>N<sub>10</sub>]<sup>2–</sup>), 167.0 (38, [C<sub>2</sub>H<sub>3</sub>N<sub>10</sub>]<sup>–</sup>), 189.0 (41, [C<sub>2</sub>H<sub>2</sub>N<sub>10</sub>Na]<sup>–</sup>), 205.0 (19, [C<sub>2</sub>H<sub>2</sub>N<sub>10</sub>NaO]<sup>3–</sup>), 259.0 (10, C<sub>2</sub>H<sub>4</sub>N<sub>10</sub>-gly), 281.0 (21, C<sub>2</sub>H<sub>3</sub>N<sub>10</sub>Na-gly); C<sub>2</sub>H<sub>3</sub>N<sub>10</sub>O<sub>0.5</sub>Na<sub>2</sub> (221.03 g mol<sup>-1</sup>) calc.: C 10.86, H 1.37, N 63.35%; found: C 11.16, H 1.61, N 63.31%.

### Synthesis of potassium 5,5'-hydrazinebistetrazolate (4)

Potassium hydroxide (0.224 g, 4.0 mmol) was dissolved in 15 mL degassed water in a Schlenk flask and reacted with **1** (0.336 g, 2.0 mmol) for 15 min under a stream of nitrogen until all material had dissolved. At this point, the flask was connected to a *Schlenk* line and the solvent was removed at reduced pressure yielding the compound as a white powder (0.568 g, 96%). The compound oxidizes readily to the yellow 5,5'-azobistetrazolate salt and was stored under nitrogen. DSC (5 °C min<sup>-1</sup>, °C): 236 (dec.); IR (KBr, cm<sup>-1</sup>)  $\tilde{\nu}$  = 3301(w), 3237(w), 1625(vw), 1561(w), 1490(m), 1469(s), 1360(s), 1345(vs), 1204(w), 1144(vw), 1130(m), 1114(w), 1081(vw), 1054(w), 1014(m), 917(s), 849(m), 768(s), 736(w), 718(m), 681(s), 606(m); Raman (400 mW, 25 °C, cm<sup>-1</sup>)  $\tilde{\nu}$  = 3305(32), 3238(16), 1562(5), 1488(90), 1473(24), 1381(29), 1362(10), 1346(6), 1281(5), 1227(6), 1208(66), 1145(11), 1131(15), 1119(17), 1078(21), 1048(100), 1016(7), 925(4), 852(8), 761(6), 733(6), 683(8), 499(6), 446(17), 393(6), 376(10), 353(41), 212(37), 170(11); <sup>1</sup>H NMR (DMSO-*d*<sub>6</sub>, 25 °C, ppm)  $\delta$  8.12 (s, 2H, NH–NH); <sup>13</sup>C NMR (DMSO-*d*<sub>6</sub>, 25 °C, ppm)  $\delta$  167.9 (2C, C<sub>ring</sub>); *m/z* (FAB<sup>–</sup>, xenon, 6 keV, glycerine matrix): 84.0 (18, [CH<sub>2</sub>N<sub>5</sub>]<sup>–</sup>), 118.0 (5, HCN-gly), 124.0 (3, [C<sub>2</sub>H<sub>2</sub>N<sub>7</sub>]<sup>–</sup>), 166.0 (8, [C<sub>2</sub>H<sub>2</sub>N<sub>10</sub>]<sup>2–</sup>), 167.1 (58, [C<sub>2</sub>H<sub>3</sub>N<sub>10</sub>]<sup>–</sup>), 204.9 (100, [C<sub>2</sub>H<sub>2</sub>N<sub>10</sub>K]<sup>–</sup>), 258.9 (9, C<sub>2</sub>H<sub>4</sub>N<sub>10</sub>-gly), 334.8 (30, [C<sub>2</sub>H<sub>4</sub>N<sub>10</sub>-C<sub>2</sub>H<sub>3</sub>N<sub>10</sub>]<sup>–</sup>), 372.8 (12, [C<sub>2</sub>H<sub>2</sub>N<sub>10</sub>K-C<sub>2</sub>H<sub>4</sub>N<sub>10</sub>]<sup>–</sup>); C<sub>2</sub>H<sub>2</sub>N<sub>10</sub>K<sub>2</sub> (243.97 g mol<sup>-1</sup>) calc.: C 9.84, H 0.83, N 57.40%; found: C 9.77, H 1.09, N 57.04%.

### Synthesis of rubidium 5,5'-hydrazinebistetrazolate (5)

Rubidium carbonate (0.460 g, 2.0 mmol) was suspended in 15 mL degassed water in a 25 mL Schlenk flask under a flow of nitrogen. **1** (0.336 g, 2.0 mmol) was added neat forming a suspension, which was carefully warmed up with a heatgun (carbon dioxide evolution was observed). The reaction mixture was stirred and gently warmed up until the gas evolution had ceased and it was shortly brought to reflux. After removing the solvent under high vacuum, the compound was obtained as a white powder in quantitative yield (0.760 g). The compound turns completely yellow after a few hours and was stored under nitrogen. Single crystals were obtained when nitrogen was blown over a freshly prepared solution of the material. DSC (5 °C min<sup>-1</sup>, °C): 230 (dec.); IR (KBr, cm<sup>-1</sup>)  $\tilde{\nu}$  = 3344(vw), 3286(m), 2933(vw), 1622(w), 1592(vw), 1530(s), 1488(w), 1468(vs), 1386(w), 1347(w), 1262(vw), 1243(vw), 1203(w), 1181(w), 1121(m), 1107(w), 1086(m), 1053(m), 1009(m), 890(s), 832(s), 782(s), 761(s), 730(m), 696(m), 637(s); Raman (400 mW, 25 °C, cm<sup>-1</sup>)  $\tilde{\nu}$  = 3351(16), 3289(34), 1539(21), 1488(69), 1409(6), 1374(18), 1349(8), 1204(34), 1183(29), 1140(10), 1122(24), 1108(13), 1088(10), 1045(100), 915(6), 833(8), 782(9), 731(8), 697(10), 641(11), 559(8), 545(6), 450(11), 387(14), 355(19), 273(6), 211(43), 159(7), 103(3); <sup>1</sup>H NMR (DMSO-*d*<sub>6</sub>, 25 °C, ppm)  $\delta$  7.94 (s, 2H, NH–NH), <sup>13</sup>C NMR (DMSO-*d*<sub>6</sub>, 25 °C, ppm)  $\delta$  167.9 (2C, C<sub>ring</sub>); *m/z* (FAB<sup>–</sup>, xenon, 6 keV, glycerine matrix): 84.0 (7, [CH<sub>2</sub>N<sub>5</sub>]<sup>–</sup>), 118.0 (3, HCN-gly), 124.1 (2, [C<sub>2</sub>H<sub>2</sub>N<sub>7</sub>]<sup>–</sup>), 166.0 (5, [C<sub>2</sub>H<sub>2</sub>N<sub>10</sub>]<sup>2–</sup>), 167.0 (35, [C<sub>2</sub>H<sub>3</sub>N<sub>10</sub>]<sup>–</sup>), 250.8 (33, [C<sub>2</sub>H<sub>2</sub>N<sub>10</sub>Rb]<sup>–</sup>), 259.0 (6, C<sub>2</sub>H<sub>4</sub>N<sub>10</sub>-gly), 342.8 (13, C<sub>2</sub>H<sub>3</sub>N<sub>10</sub>Cs-gly); C<sub>2</sub>H<sub>2</sub>N<sub>10</sub>Rb<sub>2</sub> (335.87 g mol<sup>-1</sup>) calc.: C 7.15, H 0.60, N 41.69%; found: C 7.39, H 0.74, N 42.20%.

### Synthesis of caesium 5,5'-hydrazinebistetrazolate (6)

**1** (0.336 g, 2.0 mmol) was suspended in 15 mL degassed water and reacted with caesium carbonate (0.652 g, 2.0 mmol) under a stream of nitrogen. The reaction mixture was gently warmed up to induce the formation of carbon dioxide until the gas evolution had stopped. The solvent was removed by blowing nitrogen gas over the solution producing single crystals of the caesium salt suitable for diffraction studies in quantitative yield (0.950 g). DSC (5 °C min<sup>-1</sup>, °C): 240 (dec.); IR (KBr, cm<sup>-1</sup>)  $\tilde{\nu}$  = 3232(vw), 2798(vw), 2409(vw), 2211(vw), 2072(vw), 1632(vw), 1508(w), 1473(w), 1435(vw), 1382(s), 1358(w), 1210(vw), 1180(m), 1146(m), 1107(vw), 1064(w), 1039(m), 1025(w), 798(w), 774(s), 727(vs); Raman (400 mW, 25 °C, cm<sup>-1</sup>)  $\tilde{\nu}$  = 3243(6), 3209(10), 1542(13), 1510(47), 1489(14), 1371(14), 1217(48), 1174(10), 1104(30), 1041(100), 991(10), 888(9), 767(9), 754(9), 607(6), 422(18), 363(9), 353(10), 242(40), 150(11); <sup>1</sup>H NMR (DMSO-*d*<sub>6</sub>, 25 °C, ppm)  $\delta$  6.73 (s, 2H, NH–NH), <sup>13</sup>C NMR (DMSO-*d*<sub>6</sub>, 25 °C, ppm)  $\delta$  168.3 (2C, C<sub>ring</sub>); *m/z* (FAB<sup>–</sup>, xenon, 6 keV, glycerine matrix): 84.0 (6, [CH<sub>2</sub>N<sub>5</sub>]<sup>–</sup>), 118.0 (3, HCN-gly), 124.1 (2, [C<sub>2</sub>H<sub>2</sub>N<sub>7</sub>]<sup>–</sup>), 166.0 (6, [C<sub>2</sub>H<sub>2</sub>N<sub>10</sub>]<sup>2–</sup>), 167.0 (32, [C<sub>2</sub>H<sub>3</sub>N<sub>10</sub>]<sup>–</sup>), 259.0 (8, C<sub>2</sub>H<sub>4</sub>N<sub>10</sub>-gly), 298.8 (42, [C<sub>2</sub>H<sub>2</sub>N<sub>10</sub>Cs]<sup>–</sup>), 390.8 (18, C<sub>2</sub>H<sub>3</sub>N<sub>10</sub>Cs-gly); C<sub>2</sub>H<sub>2</sub>N<sub>10</sub>Cs<sub>2</sub> (431.86 g mol<sup>-1</sup>) calc.: C 5.56, H 0.47, N 32.43%; found: C 5.56, H 0.60, N 32.47%.

## Conclusions

From this experimental study the following conclusions can be drawn: straightforward syntheses for alkali metal salts of the nitrogen-rich 5,5'-hydrazinebistetrazolate anion ( $[\text{C}_2\text{H}_2\text{N}_{10}]^{2-}$ ) are presented, which allow to obtain the compounds in high yields and purities. The new salts were characterized by analytical and spectroscopic methods and the structure of the  $[\text{C}_2\text{H}_2\text{N}_{10}]^{2-}$  anion was elucidated by means of X-ray crystal structure determination. The high nitrogen content and high thermal stability of the salts make them interesting as more environmentally friendly pyrotechnic ingredients than commonly used materials (e.g.,  $\text{Sr}(\text{ClO}_4)_2$ ). Lastly, the ready oxidation of salts of  $[\text{C}_2\text{H}_2\text{N}_{10}]^{2-}$  to form salts of  $[\text{C}_2\text{N}_{10}]^{2-}$  provides a safer procedure for the synthesis of 5,5'-azobistetrazolate salts.

## Acknowledgements

Financial support of this work by the Ludwig-Maximilian University of Munich (LMU), the Fonds der Chemischen Industrie (FCI), the European Research Office (ERO) of the U.S. Army Research Laboratory (ARL) under contract nos N 62558-05-C-0027, R&D 1284-CH-01, R&D 1285-CH-01, 9939-AN-01, W911NF-07-1-0569, W911NF-08-1-0372 and W911NF-08-1-0380 and the Bundeswehr Research Institute for Materials, Explosives, Fuels and Lubricants (WIWEB) under contract nos E/E210/4D004/X5143 and E/E210/7D002/4F088 is gratefully acknowledged. The authors are indebted to and thank Dr Betsy Rice and Dr Gary Chen for many helpful discussions and support of their work. We also acknowledge Mr Stefan Huber for help with the sensitivity tests. The authors acknowledge collaborations with Dr M. Krupka (OZM Research, Czech Republic) in the development of new testing and evaluation methods for energetic materials and with Dr M. Sućesca (Brodarski Institute, Croatia) in the development of new computational codes to predict the detonation parameters of high-nitrogen explosives.

## References

- 1 H. Birscher, *Chimia*, 2004, **58**, 355.
- 2 T. M. Klapötke and G. Steinhauser, *Angew. Chem., Int. Ed.*, 2008, **47**, 3330.
- 3 J. Köhler and R. Mayer, *Explosivstoffe*, Wiley-VCH, Weinheim, 9th edn, 1998.
- 4 T. M. Klapötke, G. Holl, J. Geith, A. Hammerl and J. J. Weigand, *Proceedings of the 7th Seminar on New Trends Research and Energy Materials*, Pardubice, Czech Republic, 2004.
- 5 G. Geisberger, T. M. Klapötke and J. Stierstorfer, *Eur. J. Inorg. Chem.*, 2007, **30**, 4743.
- 6 T. M. Klapötke, J. Stierstorfer and A. U. Wallek, *Chem. Mater.*, 2008, **20**, 4519.
- 7 M. I. Eremets, A. G. Gavriliuk, I. A. Trojan, D. A. Dzivenko and R. Boehler, *Nat. Mater.*, 2004, **3**, 558.
- 8 K. O. Christie, W. W. Wilson, J. A. Sheehy and J. A. Boatz, *Angew. Chem., Int. Ed.*, 1999, **38**, 2004; D. A. Dixon, D. Feller, K. O. Christie, W. W. Wilson, A. Vij, H. D. Vij, H. D. Brooke, R. M. Olson and M. S. Gordon, *J. Am. Chem. Soc.*, 2004, **126**, 834A. Hahma, E. Holmber, N. Hore, R. Tryman, S. Wallin and H. Östmark, *33rd International Annual Conference on ICT*, Karlsruhe, Germany, 2002, vol. 62, p. 1; A. Vij, J. G. Pavlovich, W. W. Wilson, V. Vij and K. O. Christie, *Angew. Chem., Int. Ed.*, 2002, **41**, 3051;

- S. D. Kunikeev, H. S. Taylor, T. Schroer, R. Halges, C. J. B. Jones and K. O. Christie, *Inorg. Chem.*, 2006, **45**, 437.
- 9 (a) K. Karaghiosoff, T. M. Klapötke, P. Mayer, C. Miró Sabaté, A. Penger and J. M. Welch, *Inorg. Chem.*, 2008, **47**, 1007; (b) T. M. Klapötke, P. Mayer, C. Miró Sabaté, J. M. Welch and N. Wiegand, *Inorg. Chem.*, 2008, **47**, 6014; (c) T. M. Klapötke and C. Miró Sabaté, *Chem. Mater.*, 2008, **20**, 1750; (d) T. M. Klapötke and C. Miró Sabaté, *Chem. Mater.*, 2008, **20**, 3629.
- 10 H. Xue, B. Twamley and J. M. Shreeve, *J. Mater. Chem.*, 2005, **15**, 3459; H. Xue, Y. Gao, B. Twamley and J. M. Shreeve, *Chem. Mater.*, 2005, **17**, 191; H. Xue, H. Gao, B. Twamley and J. M. Shreeve, *Chem. Mater.*, 2007, **19**, 1731; Y. Gao, H. Gao, B. Twamley and J. M. Shreeve, *Adv. Mater. (Weinheim, Ger.)*, 2007, **19**, 2884; H. Gao, C. Ye, C. M. Piekarski and J. M. Shreeve, *J. Phys. Chem. A*, 2007, **111**, 10718; Y. H. Joo, B. Twamley, S. Garg and J. M. Shreeve, *Angew. Chem., Int. Ed.*, 2008, **47**, 6236.
- 11 A. K. Sikder and N. Sikder, *J. Hazard. Mater.*, 2004, **A112**, 1.
- 12 C. Darwich, T. M. Klapötke and C. Miró Sabaté, *Propellants, Explos., Pyrotech.*, 2008, DOI: 10.1002/prep.200700216; C. Darwich, T. M. Klapötke and C. Miró Sabaté, *Chem.-Eur. J.*, 2008, **14**, 5756; T. M. Klapötke and C. Miró Sabaté, *Z. Anorg. Allg. Chem.*, 2008, **634**, 1017; Y. Huang, H. Gao, B. Twamley and J. M. Shreeve, *Eur. J. Inorg. Chem.*, 2008, 2560; Z. Zeng, R. Wang, B. Twamley, D. A. Parrish and J. M. Shreeve, *Chem. Mater.*, 2008, **20**, 6176.
- 13 T. M. Klapötke, K. Karaghiosoff, P. Mayer, A. Penger and J. M. Welch, *Propellants, Explos., Pyrotech.*, 2006, **31**, 188; T. M. Klapötke, C. Miró Sabaté and M. Rusan, *Z. Anorg. Allg. Chem.*, 2008, **634**, 688; T. M. Klapötke, C. Miró Sabaté and J. M. Welch, *Z. Anorg. Allg. Chem.*, 2008, **634**, 857.
- 14 A. Hammerl, M. A. Hiskey, G. Holl, T. M. Klapötke, K. Polborn, J. Stierstorfer and J. J. Weigand, *Chem. Mater.*, 2005, **17**, 3784; J. Stierstorfer, T. M. Klapötke, A. Hammerl and B. Chapman, *Z. Anorg. Allg. Chem.*, 2008, **634**, 1051; G. Geisberger, T. M. Klapötke and J. Stierstorfer, *Eur. J. Inorg. Chem.*, 2007, **30**, 4743; T. M. Klapötke and J. Stierstorfer, *Helv. Chim. Acta*, 2007, **90**, 2132.
- 15 R. C. West and S. M. Selby, *Handbook of Chemistry and Physics*, The Chemical Rubber Co., Cleveland, 48th edn, 1967–1968.
- 16 V. A. Ostrovskii, M. S. Pevzner, T. P. Kofman and I. V. Tselinskii, *Targets Heterocycl. Syst.*, 1999, **3**, 467.
- 17 H. Xue, B. Twamley and J. M. Shreeve, *Inorg. Chem.*, 2004, **43**, 7972; C. Ye, J. C. Xiao, B. Twamley and J. M. Shreeve, *Chem. Commun.*, 2005, **21**, 2750; R. P. Singh, R. D. Verma, D. T. Meshri and J. M. Shreeve, *Angew. Chem., Int. Ed.*, 2006, **45**, 3584.
- 18 T. M. Klapötke, P. Mayer, A. Schulz and J. J. Weigand, *Propellants, Explos., Pyrotech.*, 2004, **29**, 325; J. C. Galvez-Ruiz, G. Holl, K. Karaghiosoff, T. M. Klapötke, K. Loehnitz, P. Mayer, H. Noeth, K. Polborn, C. J. Rohbogner, M. Suter and J. J. Weigand, *Inorg. Chem.*, 2005, **44**, 5192; A. Hammerl, M. A. Hiskey, G. Holl, T. M. Klapötke, K. Polborn, J. Stierstorfer and J. J. Weigand, *Chem. Mater.*, 2005, **17**, 3784.
- 19 M. H. V. Huynh, M. A. Hiskey, T. J. Meyer and M. Wetzler, *Proc. Natl. Acad. Sci. U. S. A.*, 2006, **103**, 5409; M. H. V. Huynh, M. D. Coburn, T. J. Meyer and M. Wetzler, *Proc. Natl. Acad. Sci. U. S. A.*, 2006, **103**, 10322.
- 20 T. M. Klapötke, C. Miró Sabaté and J. M. Welch, *Dalton Trans.*, 2008, 6372.
- 21 V. Ernst, T. M. Klapötke and J. Stierstorfer, *Z. Anorg. Allg. Chem.*, 2007, **633**, 879.
- 22 A. Hammerl, G. Holl, T. M. Klapötke, P. Mayer, H. Nöth, H. Piotrowski and M. Warchhold, *Eur. J. Inorg. Chem.*, 2002, **4**, 834.
- 23 R. J. Spear and P. P. Elischer, *Aust. J. Chem.*, 1982, **35**, 1; G. O. Reddy and A. K. Chatterjee, *J. Hazard. Mater.*, 1984, **9**, 291; L. V. De Yong and G. Campanella, *J. Hazard. Mater.*, 1989, **21**, 125; A. Hammerl, G. Holl, M. Kaiser, T. M. Klapötke and H. Piotrowski, *Z. Anorg. Allg. Chem.*, 2003, **629**, 2117.
- 24 J. Thiele, *Justus Liebigs Ann. Chem.*, 1898, **303**, 57; A. Hammerl, PhD Thesis, Ludwig-Maximilian University, Munich, 2001.
- 25 T. M. Klapötke and C. Miró Sabaté, *Z. Anorg. Allg. Chem.*, 2007, **633**, 2671.
- 26 K. Karaghiosoff, T. M. Klapötke and C. Miró Sabaté, *Eur. J. Inorg. Chem.*, 2008, in press.
- 27 J. Thiele, *Justus Liebigs Ann. Chem.*, 1892, **270**, 54; J. Thiele and J. T. Marais, *Justus Liebigs Ann. Chem.*, 1893, **273**, 144; J. Thiele, *Ber. Dtsch. Chem. Ges.*, 1893, **26**, 2645.

- 28 M. J. Frisch, G. W. Trucks, H. B. Schlegel, G. E. Scuseria, M. A. Robb, J. R. Cheeseman, J. A. Montgomery, Jr, T. Vreven, K. N. Kudin, J. C. Burant, J. M. Millam, S. S. Iyengar, J. Tomasi, V. Barone, B. Mennucci, M. Cossi, G. Scalmani, N. Rega, G. A. Petersson, H. Nakatsuji, M. Hada, M. Ehara, K. Toyota, R. Fukuda, J. Hasegawa, M. Ishida, T. Nakajima, Y. Honda, O. Kitao, H. Nakai, M. Klene, X. Li, J. E. Knox, H. P. Hratchian, J. B. Cross, C. Adamo, J. Jaramillo, R. Gomperts, R. E. Stratmann, O. Yazyev, A. J. Austin, R. Cammi, C. Pomelli, J. W. Ochterski, P. Y. Ayala, K. Morokuma, G. A. Voth, P. Salvador, J. J. Dannenberg, V. G. Zakrzewski, S. Dapprich, A. D. Daniels, M. C. Strain, O. Farkas, D. K. Malick, A. D. Rabuck, K. Raghavachari, J. B. Foresman, J. V. Ortiz, Q. Cui, A. G. Baboul, S. Clifford, J. Cioslowski, B. B. Stefanov, G. Liu, A. Liashenko, P. Piskorz, I. Komaromi, R. L. Martin, D. J. Fox, T. Keith, M. A. Al-Laham, C. Y. Peng, A. Nanayakkara, M. Challacombe, P. M. W. Gill, B. Johnson, W. Chen, M. W. Wong, C. Gonzalez and J. A. Pople, *GAUSSIAN 03 (Revision B0.4)*, Gaussian, Inc., Pittsburgh, PA, 2004.
- 29 N. B. Colthup, L. H. Daly and S. E. Wiberley, *Introduction to Infrared and Raman Spectroscopy*, Academic Press, Boston, 1990.
- 30 *CrysAlis CCD*, Version 1.171.27p5 beta, Oxford Diffraction Ltd.
- 31 *CrysAlis RED*, Version 1.171.27p5 beta, Oxford Diffraction Ltd.
- 32 A. Altomare, G. Cascarano, C. Giacovazzo and A. Guagliardi, *J. Appl. Crystallogr.*, 1993, **26**, 343.
- 33 G. M. Sheldrick, *SHELXS-97, Program for Crystal Structure Solution*, University of Göttingen, Göttingen, 1994.
- 34 G. M. Sheldrick, *SHELXS-97, Program for Crystal Structure Solution*, University of Göttingen, Göttingen, 1997.
- 35 L. J. Farrugia, *J. Appl. Crystallogr.*, 1999, **32**, 837.
- 36 A. L. Spek, *PLATON, A Multipurpose Crystallographic Tool*, Utrecht, 1999.
- 37 *SCALE3 ABSPACK—An Oxford Diffraction Program*, Oxford Diffraction Ltd., 2005.
- 38 A. F. Holleman, E. Wiberg and N. Wiberg, *Lehrbuch der Anorganischen Chemie*, Walter de Gruyter, Berlin, 1995, 101st edn.
- 39 I. D. Brown, *Acta Crystallogr., Sect. B: Struct. Sci.*, 1988, **44**, 545.
- 40 J. Bernstein, R. E. Davis, L. Shimon and N. Chang, *Angew. Chem., Int. Ed. Engl.*, 1995, **34**, 1555.
- 41 <http://www.ccdc.cam.ac.uk/support/documentation/rpluto/TOC.html>.
- 42 T. M. Klapötke, C. Kuffer, P. Mayer, K. Polborn, A. Schulz and J. J. Weigand, *Inorg. Chem.*, 2005, **44**, 5949; T. M. Klapötke, H. Radies and J. Stierstorfer, *Z. Naturforsch., B: Chem. Sci.*, 2007, **62**, 1343.
- 43 A. Bondi, *J. Phys. Chem.*, 1964, **68**, 441.
- 44 <http://www.bam.de>; <http://www.reichel-partner.de/>.
- 45 NATO standardization agreement (STANAG) on explosives, impact sensitivity tests, no. 4489, Ed. 1, Sept. 17, 1999.
- 46 NATO standardization agreement (STANAG) on explosive, friction sensitivity tests, no. 4487, Ed. 1, Aug. 22, 2002.
- 47 WIWEB-Standardarbeitsanweisung 4-5.1.02, Ermittlung der Explosionsgefährlichkeit, hier der Schlagempfindlichkeit mit dem Fallhammer, Nov. 8, 2002.
- 48 WIWEB-Standardarbeitsanweisung 4-5.1.03, Ermittlung der Explosionsgefährlichkeit oder der Reibeempfindlichkeit mit dem Reibeapparat, Nov. 8, 2002.
- 49 UN Recommendations on the Transport of Dangerous Goods: Impact: Insensitive >40 J, less sensitive  $\geq 35$  J, sensitive  $\geq 4$ , very sensitive  $\leq 3$  J. Friction: insensitive >360 N, less sensitive = 360 N, sensitive <360 N and >80 N, very sensitive  $\leq 80$  N, extremely sensitive  $\leq 10$  N.
- 50 Calculation of the oxygen balance:  $\Omega(\%) = (\text{O}-2\text{C}-\text{H}/2-\text{xAO})/1600/M$ ;  $M$  = molecular mass.
- 51 NIST Chemistry WebBook, NIST Standard Reference Database Number 69-March, 2003 Release, www version: <http://webbook.nist.gov/chemistry>.
- 52 [http://www.linseis.net/html\\_en/thermal/dsc/dsc\\_pt10.php](http://www.linseis.net/html_en/thermal/dsc/dsc_pt10.php).
- 53 <http://www.perkinelmer.com>.
- 54 <http://www.parrinst.com>.